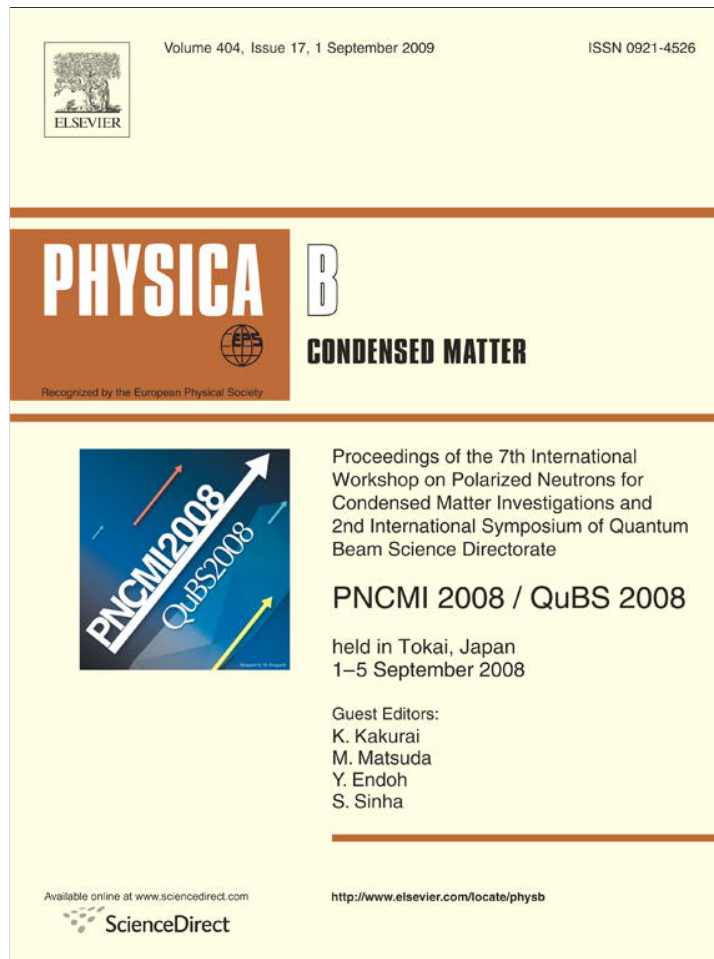


Provided for non-commercial research and education use.
Not for reproduction, distribution or commercial use.



This article appeared in a journal published by Elsevier. The attached copy is furnished to the author for internal non-commercial research and education use, including for instruction at the authors institution and sharing with colleagues.

Other uses, including reproduction and distribution, or selling or licensing copies, or posting to personal, institutional or third party websites are prohibited.

In most cases authors are permitted to post their version of the article (e.g. in Word or Tex form) to their personal website or institutional repository. Authors requiring further information regarding Elsevier's archiving and manuscript policies are encouraged to visit:

<http://www.elsevier.com/copyright>



Two-dimensional spatially ordered system of nickel nanowires probed by polarized SANS

K.S. Napolskii ^{a,*}, A.P. Chumakov ^b, S.V. Grigoriev ^b, N.A. Grigoryeva ^c, H. Eckerlebe ^d, A.A. Eliseev ^a, A.V. Lukashin ^a, Yu.D. Tretyakov ^a

^a Department of Materials Science, Moscow State University, 119992 Moscow, Russia

^b Petersburg Nuclear Physics Institute, Gatchina, 188300 St. Petersburg, Russia

^c Faculty of Physics, St-Petersburg State University, 198504 St. Petersburg, Russia

^d GKSS Forschungszentrum, 21502 Geesthacht, Germany

ARTICLE INFO

Keywords:

Anodic aluminum oxide

Magnetic nanowires

Polarized small-angle neutron diffraction

ABSTRACT

Structural and magnetic properties of two-dimensional spatially ordered system of ferromagnetic nickel nanowires embedded into Al_2O_3 matrix have been studied using polarized small-angle neutron scattering. The small-angle diffraction pattern exhibits many diffraction peaks, which corresponds to the scattering from highly correlated hexagonal structure of pores and magnetic nanowires. Magnetic contribution to the scattering has complex behavior and cannot be explained without taking into account stray fields located between magnetized nanowires.

© 2009 Elsevier B.V. All rights reserved.

The anodic oxidation method is known more than 100 years and is widely used in technology for formation of protective oxide coatings on metal surfaces. The interest of scientific community was attracted again to the process of anodic oxidation of metals about 15 years ago, when spatially ordered porous alumina films were first formed by two-stage anodization [1]. At present, anodic aluminum oxide (AAO) films are most widely used as matrices for synthesizing ordered arrays of anisotropic nanostructures of various compositions [2–4].

Small-angle neutron scattering (SANS) method is extensively used for studying spatially correlated structures, however, only a limited number of works have been performed for characterization of ordered nanomaterials and magnetic nanocomposites based on AAO [5–7]. The lack of the researcher's attention is caused by difficulties with interpretation of the data obtained by SANS. According to our recent results [5,6] the small-angle diffraction on these objects should be described by the scattering theory beyond the Born approximation. Moreover as the SANS method is sensitive to both the nuclear and magnetic structure of nanocomposites, one should find a way to extract all the contributions to scattering which is not a trivial task. In case of magnetic composites the picture could be affected by the complicated system of demagnetizing fields appeared in the sample upon magnetization process. Thus in the present study we discuss methodology for utilizing SANS to determine nuclear and magnetic structure of spatially ordered nanocomposites using

magnetic nickel nanowire arrays in porous alumina matrix as a test material.

AAO films were prepared by the two-step anodization technique [4]. The resulting porous matrices with a thickness of about 60 μm , periodicity of structure of 105 nm and the pore diameter of 40 nm were used as templates to synthesize magnetic nanowires by electroplating technique. For the controlled growth of Ni nanoparticles in the porous film, potentiostatic electrodeposition (-0.8 V vs Ag/AgCl reference electrode) was performed in a three-electrode cell using gold-coated AAO membrane as a working electrode. After 24 h growth the formation of nanowires with a length of 50 μm and a diameter of 40 nm, uniformly filling alumina matrix, was observed by SEM.

Small-angle neutron scattering measurements were carried out with the instrument SANS-2 at the Geesthacht neutron facility (GeNF). A polarized neutron beam with the polarization $P_0 = 0.95$, with a wavelength ranging from $\lambda = 0.5$ to 1.2 nm and a wavelength spread of $\Delta\lambda/\lambda = 0.1$, was used. A film with an area of 0.5 cm^2 was oriented perpendicularly to the neutron beam and was uniformly irradiated over the entire area. Such an orientation of the sample corresponds to the pore arrangement, as well as the long axis of the magnetic nanowires, to be set parallel to the incident beam. The chosen geometry of the experiment allows the observation of the diffraction pattern from the ordered structure of the pores in the small-angle scattering range. The sample-detector distances of 15 and 11 m for the neutron wavelength of 0.5–0.8 nm and of 0.8–1.2 nm, respectively, were used with appropriate collimations to cover q range from 0.025 to 0.2 nm^{-1} . An external magnetic field (up to 800 mT) was applied in the horizontal plane and perpendicular to the incident beam

* Corresponding author.

E-mail address: napolsky@inorg.chem.msu.ru (K.S. Napolskii).

(perpendicular to the long axis of the nanowires). We determined the total (nuclear and magnetic) scattering ($I(q) = I^+(q) + I^-(q)$) and the polarization dependent part of the scattering ($\Delta I(q) = I^+(q) - I^-(q)$) where $I^+(q)$ and $I^-(q)$ are the intensities for neutrons polarized parallel (+) and anti-parallel (-) to the magnetic field. The field-dependent scattering intensity was extracted as $I_H(q) = I(q, H) - I(q, 0)$.

A diffraction pattern measured from AAO membrane with embedded Ni nanowires is shown in Fig. 1a. The hexagonally arranged set of reflections demonstrates the 6-fold symmetry along the direction normal to the film surface. Rather smudged shape of reflexes should be obviously attributed to the enhancement of the quasi-randomly oriented multidomain pore structure. The momentum-transfer dependence of the radially averaged neutron scattering intensity $I(q)$ is shown in Fig. 1b. The dependence $I(q)$ is satisfactorily reproduced by the sum of the Gaussians centered at $q_{10} = 0.068 \pm 0.004 \text{ nm}^{-1}$, $q_{11} = 0.119 \pm 0.004 \text{ nm}^{-1}$, $q_{20} = 0.138 \pm 0.004 \text{ nm}^{-1}$, with a half-width $w = 0.0100 \pm 0.0005 \text{ nm}^{-1}$; and the diffuse small-angle scattering, which is represented by the Gaussian centered at $q = 0$. The obtained positions of the reflections are classified in the two-dimensional hexagonal lattice with the parameter $a = 106 \pm 2 \text{ nm}$. The wavelength dependence of the integral scattering intensity for the reflection at q_{10} is shown in Fig. 1c. The intensity decreases with increase of the wavelength proportional to λ^{-2} which accords well to theoretical predictions [5].

The magnetic field dependent component of the radially averaged neutron scattering intensity $I_H(q)$ was extracted as the difference between the magnetic cross-sections of the sample in two significantly different states: a state close to the saturation magnetization (in the field $H = 800 \text{ mT}$) and a completely demagnetized state, i.e. without magnetic prehistory at $H = 0$ (Fig. 2a). The main component of the magnetic cross-section at $H = 800 \text{ mT}$ is the ensemble of the magnetic reflections described by the sum of the Gaussians, whose positions correspond to maxima of the nuclear scattering cross-sections. On the contrary, the main component of the cross-section in zero magnetic field is scattering on domains, i.e. diffuse scattering which is described by the Gaussian at $q = 0$, thus giving no contribution to the diffraction peaks. The approximation of the experimental data in the framework of this model is shown in Fig. 2a.

The dependence $I_H(q)$ is satisfactorily reproduced by the same sum of the Gaussians as in case of the total intensity. The wavelength dependence of the integral scattering intensity for coherent scattering at q_{10} is shown in Fig. 2b. The intensity decreases with increase of the wavelength proportional to λ^{-2} in good agreement with the predictions of the theory [6] and similar to the total intensity shown in Fig. 1. On the other hand the azimuthal dependence of the magnetic scattering intensity exhibits non-trivial features. Fig. 3 shows the intensity of the magnetic scattering normalized by the total intensity denoted as $R(\alpha) = I_H(\alpha)/\Sigma I(\alpha)$ at $|q| = q_{(10)}$, where α is the azimuthal angle between the field direction \mathbf{H} and the scattering vector \mathbf{q} (see Fig. 1a).

As is well seen from Fig. 3, the magnetic scattering I_H is maximal for $\alpha = 0^\circ$ and 180° ($\mathbf{q} \parallel \mathbf{H}$) and it is minimal at $\alpha = 90^\circ$ and 270° ($\mathbf{q} \perp \mathbf{H}$). Thus, the magnetic scattering is preferable at $\mathbf{q} \parallel \mathbf{H}$ and is suppressed at $\mathbf{q} \perp \mathbf{H}$ that is opposite to the expectation that the intensity of magnetic scattering is proportional to $m_{\perp q}^2$.

The picture of the interference scattering $\Delta I(q)$ looks puzzling as well. The q -dependence of the interference contribution $\Delta I(q)$ is shown in Fig. 4 for different directions of the scattering vector $\alpha = 0^\circ, 30^\circ, 60^\circ, 90^\circ$ at $H = 800 \text{ mT}$. As is well seen the interference scattering at $q = q_{(10)}$ is maximal at $\mathbf{q} \parallel \mathbf{H}$ i.e. at $\alpha = 0^\circ$. With increase of α it decreases and changes its sign at $\alpha \sim 60^\circ$ becoming negative at $\mathbf{q} \perp \mathbf{H}$, i.e. at $\alpha = 90^\circ$. The situation is different at

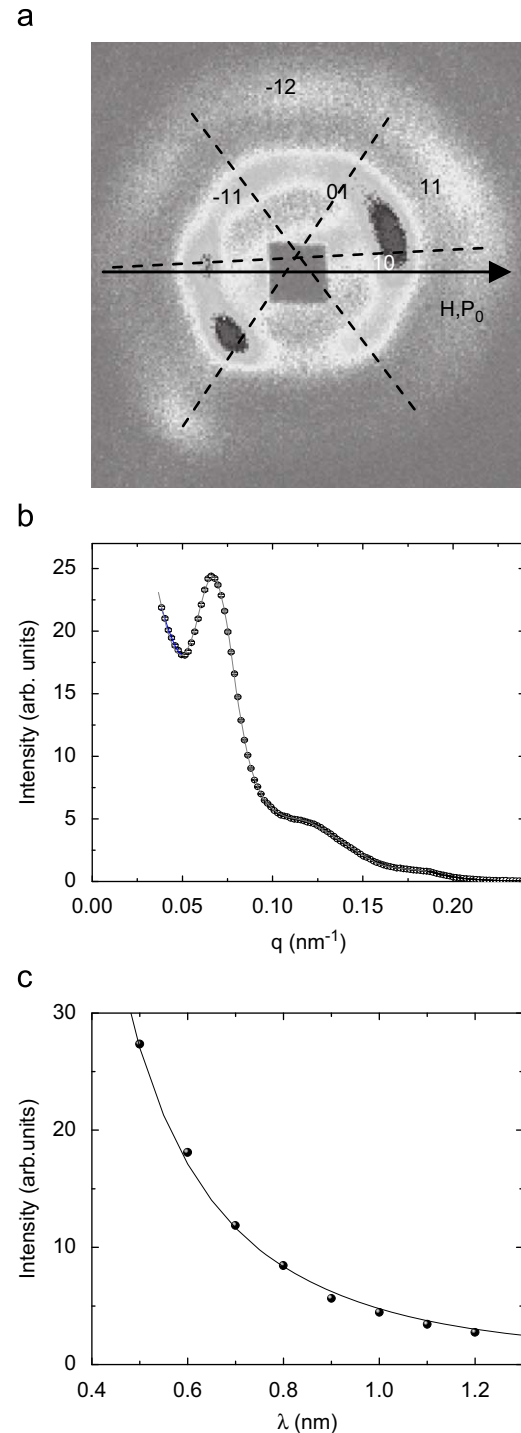


Fig. 1. (a) The two-dimensional diffraction pattern from Al_2O_3 porous film filled with Ni nanowires, (b) momentum-transfer dependence of the neutron scattering intensity at $\lambda = 0.5 \text{ nm}$ and (c) wavelength dependence of the intensity of the reflection at q_{10} .

$q \sim q_{(11)}$. No second order reflections were observed in the interference at $\alpha = 0^\circ$ and 30° , i.e. for $\mathbf{q} \parallel \mathbf{H}$. However, they become significant for $\alpha = 60^\circ$ (reflection 02) and for 90° (reflection 12). The wavelength dependence of the integral interference scattering intensity for reflections at q_{10} for $\alpha = 0^\circ$ and 90° is shown in Fig. 4b. The intensity for $\alpha = 0$ decreases with increase of the wavelength as it can be expected and similar to the total and magnetic intensity shown in Figs. 1 and 2, so does the absolute value of intensity for $\alpha = 90$, but with the negative sign.

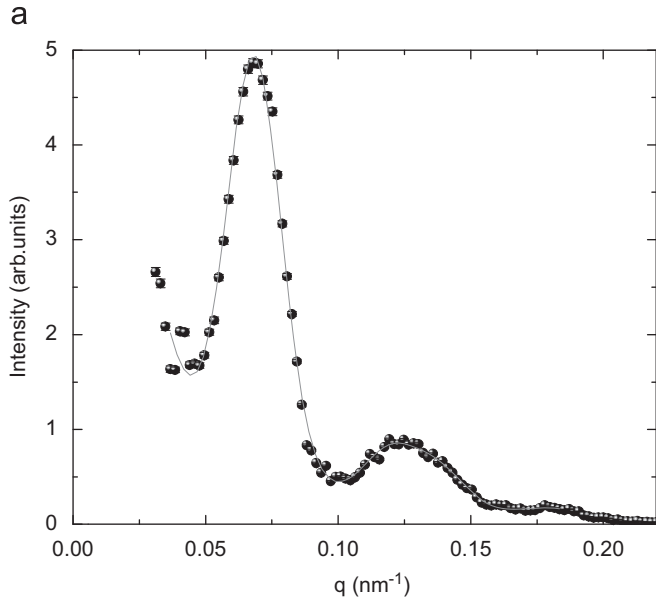


Fig. 2. (a) Momentum-transfer dependence of the magnetic neutron scattering intensity $I_H(q)$ at the wavelengths $\lambda = 0.5$ nm and (b) wavelength dependence of the intensity of the reflection at q_{10} .

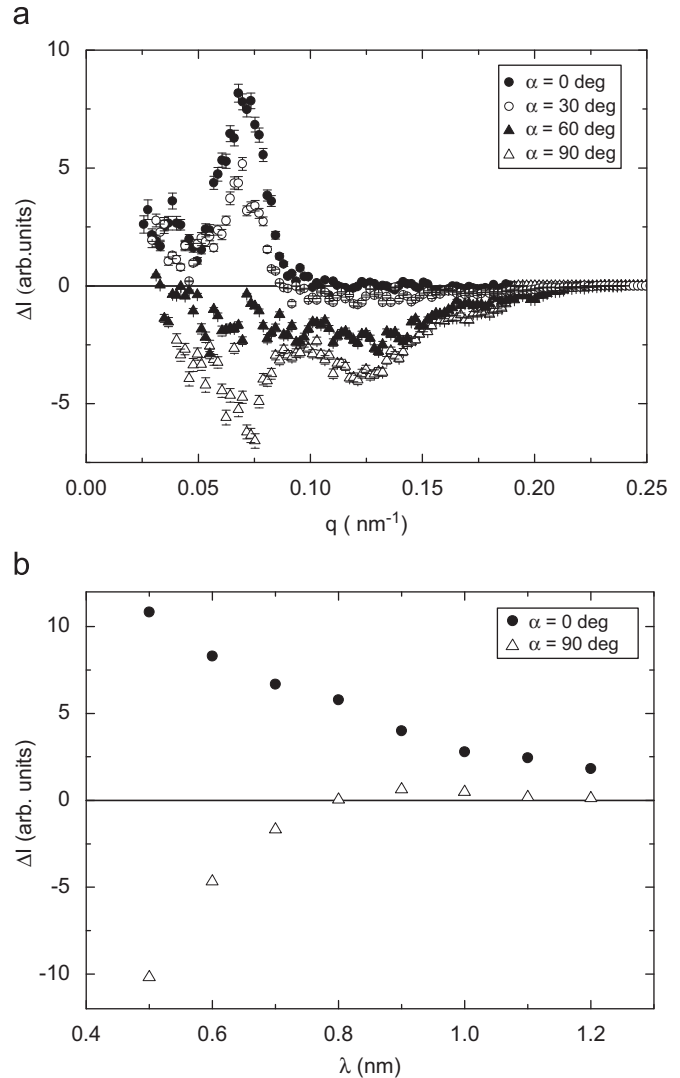


Fig. 4. (a) Momentum-transfer dependence of the interference intensity $\Delta I(q)$ at $\lambda = 0.5$ nm and for $\alpha = 0^\circ, 30^\circ, 60^\circ, 90^\circ$ and (b) wavelength dependence of the interference intensity at q_{10} for $\alpha = 0^\circ$ and 90° .

The azimuth dependence of the interference intensity at $|q| = q_{(10)}$ normalized by the total scattering intensity $[P(\alpha) = \Delta I(\alpha)/\sum I(\alpha)]$ is shown in Fig. 5. As is well seen the interference ΔI is maximal for $\alpha = 0^\circ$ and 180° and it is minimal and negative at $\alpha = 90^\circ$ and 270° .

Thus, the interference scattering is in contradiction to the theory, which predicts the term $\Delta I(\alpha)$ is proportional to $[(\mathbf{P}_0 \cdot \mathbf{m}_{\perp q}) \sim \sin^2 \alpha]$.

To satisfy the theoretical predictions one should suppose that the system of the spatially ordered magnetic nanowires in an external magnetic field produces a complicated demagnetizing field lines inside the body of the sample. These fields can be, nevertheless, divided into two magnetic subsystems: (i) the subsystem of magnetic nanowires and (ii) subsystem of the stray fields in the space between the nanowires. Both subsystems possess the spatial ordering but with magnetic lines which are differently oriented in space. A detailed model of the magnetization process will be published elsewhere.

In conclusion, (i) we have shown that the small-angle diffraction on the two-dimensional spatially ordered system of the pores or of the ferromagnetic nanowires should be described by the scattering theory beyond the Born approximation [5,6]. It is experimentally proven by the strong wavelength dependence of

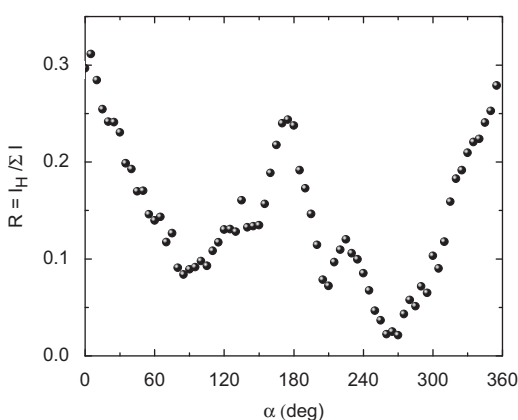


Fig. 3. Azimuth dependence of the normalized magnetic scattering intensity $R(\alpha) = I_H(\alpha)/\sum I(\alpha)$ at $|q| = q_{(10)}$ and $\lambda = 0.5$ nm.

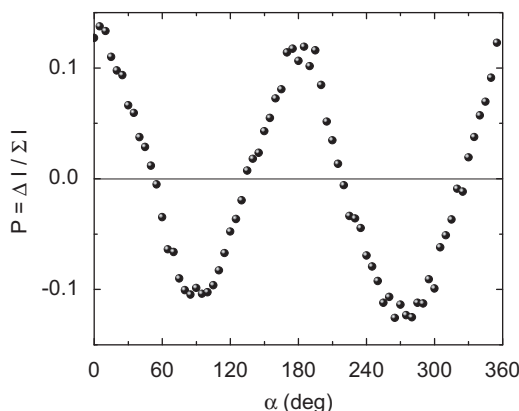


Fig. 5. Azimuth dependence of the normalized interference scattering intensity $P(\alpha) = \Delta I(\alpha)/\Sigma I(\alpha)$ at $|q| = q_{(10)}$ and $\lambda = 0.5$ nm.

the reflection's intensity, while the intensity is wavelength independent within the Born approximation. (ii) The picture of the magnetic scattering from the ordered system of the magnetic

nanowires is not satisfactory without taking into account regularly located subsystem of the stray fields enhanced upon magnetization process.

This work was performed within the framework of a Federal Special Scientific and Technical Program (projects 02.513.11.3392). The Russian authors are grateful to the GKSS Research Centre (Germany) for hospitality.

References

- [1] H. Masuda, K. Fukuda, *Science* 268 (1995) 1466.
- [2] K.S. Napolskii, A.A. Eliseev, N.V. Yesin, A.V. Lukashin, Yu.D. Tretyakov, N.A. Grigorieva, S.V. Grigoriev, H. Eckerlebe, *Physica E* 37 (2007) 178.
- [3] K.S. Napolskii, P.J. Barczuk, S.Yu. Vassiliev, A.G. Veresov, G.A. Tsirlina, P.J. Kulesza, *Electrochimica Acta* 52 (2007) 7910.
- [4] S. Shingubara, *Journal of Nanoparticle Research* 5 (2003) 17.
- [5] S.V. Grigoriev, N.A. Grigorieva, A.V. Syromyatnikov, K.S. Napolskii, A.A. Eliseev, A.V. Lukashin, Yu.D. Tretyakov, H. Eckerlebe, *JETP Letters* 85 (2007) 449.
- [6] S.V. Grigoriev, N.A. Grigorieva, A.V. Syromyatnikov, K.S. Napolskii, A.A. Eliseev, A.V. Lukashin, Yu.D. Tretyakov, H. Eckerlebe, *JETP Letters* 85 (2007) 605.
- [7] R.E. Benfield, D. Grandjean, J.C. Dore, H. Esfahanian, Z. Wu, M. Kröll, M. Geerkens, G. Schmid, *Faraday Discussions* 125 (2004) 327.